

1 **Titan’s Global Radiant Energy Budget During the Cassini Epoch (2004-2017)**

2 Ellen C. Creecy¹, Liming Li^{2*}, Xun. Jiang¹, Robert A. West³, Patrick. M. Fry⁴,

3 Conor A. Nixon⁵, Matthew E. Kenyon³, **Benoît Seignovert**⁶

4 ¹ Department of Earth and Atmospheric Sciences, University of Houston, Houston, TX, 77004.

5 ² Department of Physics, University of Houston, Houston, TX, 77004.

6 ³ Jet Propulsion Laboratory, California Institute of Technology, Pasadena, CA, 91109.

7 ⁴ Space Science and Engineering Center, University of Wisconsin-Madison, Madison, WI,
8 53706.

9 ⁵ NASA Goddard Space Flight Center, Greenbelt, MD, 20771.

10 ⁶ Université de Nantes, Univ Angers, CNRS, LPG, UMR 6112, F-44000 Nantes, France

11 *To whom all correspondence should be addressed. E-mail: lli7@central.uh.edu

12

13

14

15

16

17

18

19

20

21

22

23

24

25 Key Points:

26 Main Point 1: With Cassini multi-instrument observations (CIRS, ISS, and VMIS), we provide
27 measurements of the seasonal variations of Titan's Bond albedo.

28

29 Main Point 2: Our measurements suggest a net energy excess ($2.9\pm 0.8\%$ of the emitted energy)
30 over the Cassini era (2004-2017) on Titan.

31

32 Main Point 3: The energy imbalance changes from an energy excess ($10.7\pm 0.7\%$) in 2004-05 to
33 an energy deficit ($-3.4\pm 0.6\%$) in 2017.

34

35

36 **Abstract**

37 **Radiant energies of planets and moons are of wide interest in the fields of geoscience**
38 **and planetary science. Based on long-term multi-instrument observations from the Cassini**
39 **spacecraft, we provide here the first observational study of Titan's global radiant energy**
40 **budget and its seasonal variations. Our results show that Titan's radiant energy budget is**
41 **not balanced over the Cassini era (2004-2017) with the absorbed solar energy**
42 **$(1.208\pm 0.008)\times 10^{23}$ J larger than the emitted thermal energy $(1.174\pm 0.005)\times 10^{23}$ J. The**
43 **energy imbalance is $2.9\pm 0.8\%$ of the emitted thermal energy. Titan's global radiant energy**
44 **budget is not balanced either at the time scales of Earth's years and Titan's seasons. In**
45 **particular, the energy imbalance can be beyond 10% of the emitted thermal energy at the**
46 **time scale of an Earth year. The energy imbalance revealed in this study has important**
47 **impacts on Titan, which should be examined further by theories and models.**

48

49 **Plain Language Summary**

50 The radiant energy budget is a fundamental metric for planets and moons. Using the
51 observations from the Cassini spacecraft, we first look at Titan’s global radiant energy budget and
52 its seasonal variations. Our study suggests Titan’s global radiant energy budget is not balanced at
53 the time scales of Earth years and Titan’s seasons. The energy imbalance can help us better
54 understand the characteristics of Titan (e.g., seasonal variations). Titan’s energy imbalance also
55 suggests that it is possible that there are more terrestrial planets and moons having unbalanced
56 radiation budgets. Finally, Titan’s time-varying radiant energies imply that the internal heat of the
57 giant planets needs to be re-examined by considering the temporal variations of radiant energies.

58 **1. Introduction**

59 The radiant energy budget of a planet or a moon, which is determined by the absorbed solar
60 energy and the emitted thermal energy (Conrath et al., 1989), plays a critical role in determining
61 thermal characteristics of the astronomical body. Such a radiant energy budget can help us
62 understand the geology of terrestrial planets (e.g., polar ices of Mars) (McCleese et al., 2007),
63 internal heat related to the formation and evolution of giant planets (e.g., Smoluchowski, 1967;
64 Hubbard, 1980), and sub-surface intrinsic heat driving the jet plumes on some moons (e.g., Howett
65 et al., 2011; Spencer and Nimmo, 2013). For terrestrial bodies with atmospheres, the radiant energy
66 budget at the top of atmosphere also sets critical boundary conditions for the atmospheric systems
67 (Peixoto and Oort, 1992). The transfer and distribution of radiant energies (i.e., the absorbed solar
68 energy and the emitted thermal energy) within the atmospheric systems modify the thermal
69 structure to generate available potential energy. The available potential energy can be converted

70 into kinetic energy to drive atmospheric circulation and the related weather and climate (e.g.,
71 Lorenz, 1955; Schubert and Mitchell, 2013; Read et al., 2016).

72 Currently, Earth and Titan are the only two astronomical bodies with significant
73 atmospheres and surface seas in our solar system. For our home planet, some recent studies
74 (Hensene et al., 2005; Trenberth et al., 2016) revealed a small energy imbalance: the absorbed
75 solar energy exceeds the emitted thermal energy by a magnitude of 0.2-0.4% of the emitted energy.
76 These studies further suggest that the small energy imbalance is related to global warming and
77 climate change on Earth. Compared with numerous studies of the radiant energy budget on our
78 home planet, observational studies of Titan's global radiation budget are relatively lacking. Titan
79 is similar to Earth in many ways (e.g., surface pressure, liquid lakes/oceans on the surface, and
80 greenhouse atmosphere). On the other hand, the orbit around the Sun is much more elliptical for
81 Titan (eccentricity ~ 0.057) than for Earth (eccentricity ~ 0.017). Titan's large eccentricity means
82 that the solar flux at Titan varies beyond 20% on its orbital path. Therefore, Titan probably has a
83 much more dynamical radiant energy budget than that of Earth. Here, we want to examine the
84 temporal variations of Titan's radiant energy budget to see if there is any energy imbalance.

85 The Cassini spacecraft (Jaffe and Herrell, 1997) was an international orbiter that explored
86 the Saturn system including Titan from 2004 to 2017. The Cassini multi-instrument observations
87 have made it possible to precisely examine the global radiant energy budget of Titan for the first
88 time. In this study, we use observations from the Imaging Science Sub-system (ISS) (Porco et al.,
89 2004) and the Visual and Infrared Mapping Spectrometer (VIMS) (Brown et al., 2004) to examine
90 Titan's Bond albedo, which is defined as defined as the ratio between the reflected (or scattered)
91 solar radiation and the incident solar radiation. At each wavelength, we further define such a ratio
92 as monochromatic Bond albedo (Li et al., 2018). The Cassini ISS observations were used to

93 examine different behaviors of Titan’s reflected solar irradiance between low and high phase
94 angles (Garcia Munoz et al., 2018), but Titan’s Bond albedo and its temporal variations in the
95 Cassini epoch have not been examined yet. The Cassini ISS and VIMS observations have many
96 advantages over previous observations (e.g., better spatial resolution, better coverage of phase
97 angle, and better coverage of wavelength) (Li et al., 2010, 2011, 2018; Creecy et al., 2019), so we
98 expect to get the best measurements of Titan’s Bond albedo and hence the absorbed solar power.
99 Combined with our measurements of Titan’s emitted thermal power (Creecy et al., 2019), we can
100 determine Titan’s global radiant energy budget. Furthermore, long-term Cassini observations
101 (2004-2017) provide a great opportunity to take a first look at the seasonal variations of Titan’s
102 radiant energy budget.

103 The methodology of computing Titan’s Bond albedo and hence the absorbed solar power
104 is briefly introduced in the section of Materials and Methods. The Cassini observations and the
105 other data sets used in this study are introduced and summarized in Supporting Information Table
106 S1 and Figs. S1-S7. Titan’s troposphere and stratosphere, which play dominant roles in absorbing
107 the solar irradiance, extend to a few hundred kilometers. Therefore, Titan’s optical radius in which
108 the solar irradiance is effectively absorbed and reflected (i.e., effective radius) is substantially
109 larger than its solid radius (~ 2575 km) (Zebker et al., 2009). The effective radius, which varies
110 with wavelength, is discussed in detail in the Supporting Information (Figs. S8-S15). We basically
111 follow a method from a previous study (Smith, 1980), in which the maximal radiance contrast is
112 used to determine the edge of the effective radius. We first validate the method using Cassini
113 observations of Enceladus (Fig. S8). Then we apply the method to measure Titan’s effective radius
114 as a function of wavelength (Figs. S9-S12), which are consistent with previous observational and
115 theoretical studies (Figs. S13-S15).

116 We then calculate Titan's full-disk albedo by integrating the ISS and VIMS calibrated
117 radiance over the disks with the effective radii, which is also discussed in Supporting Information
118 (Figs. S16-S31). The comparison of Titan's full-disk albedo between the ISS and VIMS analyses
119 (Fig. S16) suggests that the two instruments provide consistent results. We also conduct the
120 comparisons of Titan's full-disk albedo between the Cassini analyses and previous analyses based
121 on other observations (Figs. S17-S19), which also validate the Cassini analyses. After validating
122 the computation of full-disk albedo, we organize the Cassini data in the two-dimensional domain
123 of time and phase angle (Fig. S20). There are observational gaps in phase angle and wavelength
124 in the Cassini ISS and VIMS observations, and we use least-squares fitting (Belington and
125 Robinson, 2003; Li et al., 2018) to fill in the observational gaps (Figs. S21-S29). Then, we obtain
126 Titan's full-disk albedo in the two-dimensional domain with complete coverage of phase angle
127 and wavelength for each year from 2004-05 to 2017 (Fig. S30). Finally, we have the
128 monochromatic geometric albedo, the monochromatic phase integral, and the monochromatic
129 Bond albedo at each wavelength for the Cassini epoch (Fig. S31). Based on the distribution of the
130 monochromatic Bond albedo (Fig. S31), we can compute Titan's Bond albedo by weighting the
131 monochromatic Bond albedo with the solar spectral irradiance.

132 The uncertainties in the measurements of Titan's Bond albedo and hence the absorbed solar
133 power mainly come from the calibration errors of the Cassini ISS and VIMS data, the uncertainties
134 related to filling the observational gaps, and the uncertainties in determining Titan's effective radii
135 at different wavelengths. We discuss these uncertainties in Supporting Information (Figs. S32-
136 S47). We also discuss the uncertainties of Titan's emitted power (the other component of Titan's
137 radiant energy budget), even though such uncertainties were already investigated in our previous
138 studies of Titan's emitted power (Li et al., 2011; Creedy et al., 2019). It should be mentioned that

139 we have consider all possible uncertainty sources to the best of our ability but it is still possible
140 that there are more uncertainty sources.

141

142 **Results**

143 Figure 1 shows Titan's Bond albedo during the Cassini epoch. Titan's Bond albedo
144 continuously decreased from 0.264 ± 0.003 in 2004-05 to 0.252 ± 0.002 in 2010 by a percentage
145 change of $4.6 \pm 1.4\%$. After that, it increased from 0.252 ± 0.002 in 2010 to 0.265 ± 0.003 in 2017 by
146 $5.2 \pm 1.4\%$. The non-monotonic variation of Bond albedo is probably related to the 15-year
147 oscillations of Titan's full-disk albedo examined in limited wavelengths (e.g., Younkin, 1974; Neff
148 et al., 1985). Furthermore, the non-monotonic variation makes Titan's Bond albedo slightly
149 increase by $0.4 \pm 1.6\%$ during the Cassini epoch.

150 Titan's Bond albedo was measured in previous studies (Younkin, 1974; Neff et al., 1985),
151 but these studies were based on observations with very limited coverage of wavelength and phase
152 angle. The Cassini observations are much better than these previous observations, so the analysis
153 based on the Cassini observations provides improved measurements of Titan's Bond albedo. The
154 temporal variations of Titan's monochromic Bond albedos at some wavelengths were explored in
155 previous studies (Sromovsky et al., 1981; Lockwood and Thompson, 2009), but the investigations
156 of the temporal variations of Titan's Bond albedo had not been done before. The Cassini long-term
157 observations provide the first examination of the seasonal variations of Titan's Bond albedo and
158 hence the radiant energy budget.

159 Combining Titan's measured Bond albedo and the known solar power at Titan, we can
160 compute the total reflected solar power and the total absorbed solar power, which are shown in
161 Fig. 2. The total solar power at Titan continuously decreased $\sim 18.6\%$ from 4.307×10^{14} W in 2004-

162 05 to 3.508×10^{14} W in 2017, which is much stronger than the temporal variations of Bond albedo
163 shown in Fig. 1. The temporal variations of the total reflected solar power (panel B) and the total
164 absorbed solar power (panel C) basically follow similar variations of the total solar power (panel
165 A). The total reflected solar power continuously decreased by $18.1 \pm 1.4\%$ from
166 $(1.136 \pm 0.013) \times 10^{14}$ W in 2004-05 to $(0.930 \pm 0.010) \times 10^{14}$ W in 2017. Correspondingly, the total
167 absorbed solar power decreased by $18.7 \pm 0.5\%$ from $(3.170 \pm 0.013) \times 10^{14}$ W in 2004-05 to
168 $(2.577 \pm 0.010) \times 10^{14}$ W in 2017.

169 Figure 3 shows the comparison between the absorbed power from this study and the
170 emitted power measured in our previous study (Creedy et al., 2019). The decrease in the absorbed
171 power ($18.7 \pm 0.5\%$) is much stronger than the decrease of emitted power ($6.8 \pm 0.4\%$) for the Cassini
172 epoch. The ratio between the net radiant energy (i.e., the absorbed power – the emitted power) and
173 the emitted power changed from $10.7 \pm 0.7\%$ in 2004-05 to $-3.4 \pm 0.6\%$ in 2017. Therefore, Titan’s
174 radiant energy budget is significantly dynamic. There is an energy excess (i.e., the absorbed solar
175 energy > the emitted thermal energy) at some seasons and an energy deficit (i.e., the absorbed solar
176 power < the emitted thermal power) at other seasons. At the time scale of an Earth year, the radiant
177 energy imbalance can be more than 10% sometimes (e.g., 2005). Titan’s significant energy deficit
178 and excess at the relatively short time scales (e.g., an Earth year and a season) are caused by its
179 large orbit eccentricity (~ 0.057), and hence largely varying distance between Titan and the Sun.
180 With the varying distance, the solar flux changes quickly (solar flux is proportional to $1/r^2$, where
181 r is the distance between Titan and the Sun). The combination of the dramatic change of solar flux
182 and the relatively weak variation of Bond albedo (Fig. 2) means that the absorbed solar power
183 varies strongly. On the other hand, the temporal variation of the emitted power is relatively weak
184 because of the large thermal inertial and long radiative time constant of the atmospheric layers

185 mainly contributing to Titan's emitted power (Li et al., 2011; Creedy et al., 2019). The change of
186 emitted power cannot match the change in the absorbed solar power at the time scales of Earth
187 years and Titan's seasons. Therefore, the energy deficit and excess occur in these time scales.

188 We also integrate the absorbed solar power and the emitted thermal power over the time
189 period of 2004-2017 to get the total absorbed solar energy and the total emitted thermal energy
190 during the Cassini epoch. The total absorbed solar energy $(1.208 \pm 0.008) \times 10^{23}$ J is larger than the
191 total emitted thermal energy $(1.174 \pm 0.005) \times 10^{23}$ J, which suggests that they are not balanced even
192 for the Cassini epoch. The difference between the two energies $((0.034 \pm 0.009) \times 10^{23}$ J) is $2.9 \pm 0.8\%$
193 of the total emitted thermal energy.

194 The Cassini observational time (~ 14 years) is about one half of Titan's year (~ 29.424
195 years). To gain further insight of the annual radiant energy budget of Titan, we extrapolate the
196 Cassini results to a complete Titan year by fitting the observed absorbed and emitted powers with
197 an assumption that the seasonal cycles of the absorbed and emitted powers follow sine functions
198 (Fig. S48 in Supporting Information). Such fitting suggests an even larger energy imbalance
199 ($5.0 \pm 2.1\%$ of the total emitted thermal energy) between the total absorbed solar energy and the
200 total emitted thermal energy over a complete Titan year. However, the extrapolated result should
201 be used with caution. First, it is likely that Titan's radiant energies (especially the emitted thermal
202 energy) do not follow simple sinusoidal functions. Second, the Cassini observations show that
203 Titan's emitted power has significant fluctuation with time (Fig. 3) and we cannot rule out that
204 such fluctuation is even stronger at the times outside the Cassini epoch.

205

206 **Discussion**

207 Whether or not Titan’s radiant energy budget is balanced in a Titan year or longer times,
208 the Cassini observations suggest that Titan’s radiant energy budget is not balanced at the time
209 scales of Earth years and Titan’s seasons. In particular, the energy imbalance can be beyond 10%
210 at the time scale of Earth years (Fig. 3). Such a large energy imbalance will significantly affect
211 Titan’s atmospheric circulation and weather. To better characterize the effects of the energy
212 imbalance on Titan’s atmosphere and surface, we need further information (e.g., the vertical and
213 meridional distributions of the energy imbalance inside atmosphere and possible energy imbalance
214 at the surface). Considering that the stratospheric hazes play important roles in Titan’s radiant
215 energy budget (e.g., Read et al., 2016) and the stratosphere has a relatively short radiative time
216 constant (Flasar et al., 1981; Bezdard et al., 2018), the energy imbalance would trigger some quick
217 responses (e.g., warming) of Titan’s stratosphere if the revealed energy imbalance mainly happens
218 in the stratosphere. The radiative time constants can be longer than a Titan year for Titan’s lower
219 troposphere (Bezdard et al., 2018), so the response will take longer time if the energy imbalance
220 mainly happens in the troposphere. It is also possible that the energy imbalance can reach the
221 surface and affect its thermal characteristics.

222 The responses of Titan’s atmosphere and surface to the energy imbalance can help warm
223 up Titan’s atmosphere (or surface) and hence increase Titan’s emitted power, which can
224 potentially serve as a restoring force to help equilibrate the radiant energy budget after the Cassini
225 epoch. It is hard to estimate Titan’s response time due to lacking information on the vertical
226 distribution of energy imbalance. In addition, we do not know if the responses are strong enough
227 to compensate the energy imbalance during the Cassini epoch to equilibrate Titan’s radiant energy
228 budget. We cannot rule out the possibility that Titan’s energy imbalance exists at time scales of a
229 Titan year and even longer. If Titan has an energy imbalance at long time scales, such an energy

230 imbalance can contribute to climate change, similar to what happens on Earth. On Earth, oceans
231 are the main reservoir for the radiant energy imbalance (Hansen et al., 2005; Levitus et al., 2000).
232 On Titan, the hazes in the atmosphere are significant absorbers of solar irradiance (Read et al.,
233 2016). These hazes along with Titan's surface that has lakes/oceans both can possibly serve as the
234 reservoir for the radiant energy imbalance.

235 If the energy imbalance at the time scales of a Titan year and longer really exists on Titan,
236 a question should be asked: what is the cause of such an imbalance? Compared to the seasonal
237 variations of solar flux at Titan (Fig. 2), the temporal variations of Titan's Bond albedo are small
238 (Fig. 1), so the absorbed solar power basically follows the seasonal variations of solar flux (Fig.
239 2). The comparison of Titan's full-disk Bond albedo between the Cassini observations and the
240 observations before the Cassini epoch (Younkin, 1974; Neff et al., 1985) suggests that Titan's
241 Bond albedo is relatively stable with time even though cloud bands can modify Titan's regional
242 albedo (see Fig. S, so we expect that the temporal variations of Titan's absorbed solar power will
243 basically follow the seasonal cycle of solar flux even at time scales longer than one Titan year. In
244 other words, Titan's absorbed solar power has stable periodic variations. So the energy imbalance
245 revealed in the Cassini epoch and the possible long-term energy imbalance most likely come from
246 the behaviors of emitted power. The hazes and greenhouse gases play important roles in modifying
247 the thermal structure of Titan's atmosphere and surface by anti-greenhouse and greenhouse effects
248 (McKay et al, 1991), respectively. The hazes and the greenhouse gases vary at Titan's seasons
249 (Aharonson et al., 2009; West et al., 2018) and longer time scales (Lorenz et al., 1997), in which
250 the temporal variations of haze distribution and methane abundance are driven by not only the
251 eccentricity of Titan's orbit around the Sun but also the long-term interaction between Titan's
252 atmosphere and surface. Some of the strong temporal variations can potentially modify Titan's

253 thermal structure and hence the emitted power to a certain extent and dis-equilibrate Titan's radiant
254 energy budget. It should be mentioned that it is still possible there are other unidentified factors,
255 which can trigger and/or maintain the possible long-term energy imbalance on Titan.

256 The energy imbalance revealed in this study can help us better understand the roles of
257 Titan's radiant energy budget in the system of Titan. Due to lacking observation, an assumption
258 of a balanced radiant energy budget is used in the current theories and models (e.g., Schubert and
259 Mitchell, 2013; Read et al., 2016; Goody, 2007). It will be useful for theories and models of Titan's
260 atmosphere and climate (e.g., Newman et al., 2011; Lebonnois et al., 2012; Lora et al., 2015) to
261 examine the impacts of the revealed energy imbalance at the time scales of Earth years and Titan's
262 seasons on Titan's seasonal variations and the related processes. The analysis of Titan's radiant
263 energy budget also suggests that it is possible that there are more terrestrial planets and moons
264 having unbalanced radiant energy budgets at different time scales. There are relatively few
265 observations and studies for the radiant energy budgets of the planets and moons other than Earth
266 and Titan. The global radiant energy budgets of Mars and Venus are assumed to be balanced in
267 current theories and models (e.g., Schubert and Mitchell, 2013; Read et al., 2016; Goody, 2007),
268 but our Titan results show it is important to examine this assumption. Considering the importance
269 of the radiant energy budget and the critical roles of the possible energy imbalance in climate
270 change, we propose more missions and observations to measure the radiant energy budgets of
271 terrestrial planets and moons.

272 Finally, the temporal variations of Titan's radiant energy budget illustrate that the radiant
273 energy budget is a dynamic process. Most of the previous measurements of the radiant energy
274 budgets of planets and moons are based on snapshot observations, and the temporal variations of
275 the radiant energies were not adequately addressed. Our analyses suggest that the temporal

276 variations of radiated energies must be considered when examining the radiant energy budget
277 especially for the planets and moons with relatively large eccentricities. The radiant energy budget
278 has also been used to estimate the internal heat on the giant planets (Conrath et al., 1989), but the
279 temporal variations of radiant energies have not been considered yet for the estimates of the
280 internal heat. That means the internal heat of the giant planets needs to be critically examined by
281 considering the temporal variations of the radiant energies.

282

283

284 **Acknowledgements**

285

286 The author - Liming Li wants to thank his postdoc advisors – Dr. Barney J. Conrath and
287 Dr. Peter J. Gierasch, who encouraged him to conduct the studies of the radiant energy budgets of
288 giant planets and their moons. The great data sets recorded and processed by the Cassini CIRS,
289 ISS, UVIS, and VIMS teams make it possible for our analysis. In addition, we gratefully
290 acknowledge Dr. Erich Karkoschka and Dr. Antonio Garcia Munoz for providing the data from
291 the ground-based observatories and the Pioneer spacecraft, respectively. We also appreciate the
292 support from the NASA ROSES Cassini Data Analysis Program.

293

294 **Open Research**

295 The Cassini raw data used in this study are publicly available from NASA Planetary Data System
296 (https://pds-atmospheres.nmsu.edu/data_and_services/atmospheres_data/Cassini/Cassini.html).

297 In particular, the Cassini Imaging Science Sub-system (ISS) and Visual and Infrared Mapping
298 Spectrometer (VIMS) data sets, which are analyzed in this study, can be downloaded from
299 <https://pds-imaging.jpl.nasa.gov/volumes/iss.html> and

300 <https://pds-imaging.jpl.nasa.gov/volumes/vims.html>, respectively. The information of the ISS and
301 VIMS instrument onboard the Cassini spacecraft and the data products of the two instruments are
302 described in detail in two papers by Porco et al., 2004 (doi.org/10.1007/s11214-004-1456-7) and
303 Brown et al., 2004 (doi.org/10.1007/s11214-004-1453-x), respectively.

304

305

306 **References**

307 Aharonson, O., Hayes, A.G., Lunine, J.I., Lorenz, R.D., Allison, M.D. and Elachi, C. (2009). An
308 asymmetric distribution of lakes on Titan as a possible consequence of orbital forcing. *Nature*
309 *Geoscience* 2, 851-854.

310

311 Ajello J. M. et al. (2008). Titan airglow spectra from the Cassini Ultraviolet Imaging Spectrograph:
312 FUV disk analysis. *Geophysical research letters* 35, L06102.

313

314 Baines K. H. et al. (2005). The atmospheres of Saturn and Titan in the near-infrared: First results
315 of Cassini/VIMS. *Earth, Moon, and Planets* 96, 119-147.

316

317 Bevington, P. R. & Robinson, D. K. (2003). Data Reduction and Error Analysis for the Physical
318 Sciences, 3rd ed. (McGraw-Hill).

319

320 Bézard, B., Vinatier, S. and Achterberg, R. K. (2018). Seasonal radiative modeling of Titan's
321 stratospheric temperatures at low latitudes. *Icarus* 302, 437-450.

322

323 Brown, R. H. et al. (2004). The Cassini visual and infrared mapping spectrometer (VIMS)
324 investigation, *Space Sci. Rev.* 115, 111-168.
325

326 Buratti B. J. et al. (2010). Cassini spectra and photometry 0.25–5.1 μm of the small inner
327 moons of Saturn. *Icarus* 206, 524-536.
328

329 Conrath, B. J., Hanel, R. A. & Samuelson, R. E. (1989). Thermal Structure and Heat Balance of
330 the Outer Planets. In *Origin and Evolution of Planetary and Satellite Atmospheres* (eds. Atreya,
331 S. K., Pollack, J. B., & Matthews, M. S.) (The University of Arizona Press).
332

333 Cours, T., Cordier, D., Seignovert, B., Maltagliati, L., Biennier, L. (2020). The 3.4 μm absorption
334 in Titan's stratosphere: Contribution of ethane, propane, butane and complex hydrogenated
335 organics. *Icarus* 339, 113571.
336

337 Creecy, E. C., Li, L., Jiang, X., Nixon, C. A., West, R. A. & Kenyon, M. E. (2019). Seasonal
338 Variations of Titan's Brightness. *Geophysical Research Letters* 46, 13649-13657.
339

340 Esposito, L. W. et al. (2004). The Cassini ultraviolet imaging spectrograph investigation. *Space*
341 *science reviews* 115, 299-361.
342

343 Filacchione, G. et al. (2007). Saturn's icy satellites investigated by Cassini-VIMS: I. Full-disk
344 properties: 350–5100 nm reflectance spectra and phase curves. *Icarus* 186, 259-290.
345

346 Flasar, F. M., Samuelson, R. E., Conrath, B. J. (1981). Titan's atmosphere: Temperature and
347 dynamics. *Nature* 292, 693–698.

348

349 Flasar, F. M. et al. (2004). Exploring the Saturn system in the thermal infrared: The Composite
350 Infrared Spectrometer. *Space Sci. Rev.* 115, 169–297.

351

352 Garcia Muñoz, A. G., Lavvas, P. & West, R. A. (2017). Titan brighter at twilight than in daylight.
353 *Nature Astronomy* 1, 1-7.

354

355 Goody, R. (2007). Maximum entropy production in climate theory. *Journal of the atmospheric*
356 *sciences* 64, 2735-2739.

357

358 Hansen, J. et al. (2005). Earth's energy imbalance: confirmation and implications. *Science* 308,
359 1431-1435.

360

361 Hapke, B. (2002). Bidirectional reflectance spectroscopy: 5. The coherent backscatter opposition
362 effect and anisotropic scattering. *Icarus* 157, 523-534.

363

364 Henyey, L.G. & Greenstein, J. L. (1941). Diffuse radiation in the galaxy. *The Astrophysical*
365 *Journal* 93, 70-83.

366

367 Howett, C. J. A., Spencer, J. R., Pearl, J. & Segura, M. (2011). High heat flow from Enceladus'
368 south polar region measured using 10-600 cm⁻¹ Cassini/CIRS data. *Journal of Geophysical*
369 *Research* 116, E03003.

370

371 Hubbard, W. B. (1980). Intrinsic luminosities of the Jovian planets. *Reviews of Geophysics* 18, 1-
372 9.

373

374 Jacobowitz, H., Smith, W. L., Howell, H. B., Nagle, F. W., Hickey, J. R. (1979). The first 18
375 months of planetary radiation budget measurements from the Nimbus 6 ERB experiment. *Journal*
376 *of the Atmospheric Sciences* 36, 501-507.

377

378 Jaffe, L. D., and Herrell, L. M. (1997). Cassini/Huygens Science Instruments, Spacecraft, and
379 Mission. *Journal of Spacecraft and Rockets* 34, 509-521.

380

381 Karkoschka, E. (1994) Spectrophotometry of the jovian planets and Titan at 300-to 1000-nm
382 wavelength: The methane spectrum. *Icarus* 111, 174-192.

383

384 Karkoschka, E. (1998). Methane, Ammonia, and Temperature Measurements of the Jovian Planets
385 and Titan from CCD-Spectrophotometry. *Icarus* 133, 134-146.

386

387 Knowles, B. et al. (2020). End-mission calibration of the Cassini Imaging Science Subsystem.
388 *Planetary and Space Science* 185.

389

390 Lean, J. L., Rind, D. H. (2009). How will Earth's surface temperature change in future decades?
391 *Geophysical Research Letters* 36.
392
393 Lebonnois, S., Burgalat, J., Rannou, P., Charnay, B. (2012). Titan global climate model: A new 3-
394 dimensional version of the IPSL Titan GCM. *Icarus* 218, 707– 722.
395
396 Levitus, S., Antonov, J. I., Boyer, T. P. and Stephens, C. (2000). Warming of the world ocean.
397 *Science* 287, 2225-2229.
398
399 Li, L., Conrath, B. J., Gierasch, P. J., Achterberg, R. K., Nixon, C. A., Simon-Miller, A. A., Flasar,
400 F. M., Banfield, D., Baines, K. H., West, R. A., Ingersoll, A. P., Vasavada, A. R., Del Genio, A.
401 D., Porco, C. C., Mamoutkine, A. A., Segura, M. E., Bjoraker, G. L., Orton, G. S., Fletcher, L. N.,
402 Irwin, P. G. J. & Read, P. L. (2010). Emitted power of Saturn. *Journal of Geophysical Research -*
403 *Planet* 115, art. No. E11002.
404
405 Li, L. et al. (2011). The Global Energy Balance of Titan. *Geophys. Res. Lett.* 38, L23201.
406
407 Li, L. et al. (2018). Less absorbed solar energy and more internal heat for Jupiter. *Nature*
408 *communications* 9, 3709.
409
410 Lockwood, G. W. & Thompson, D. T. (2009). Seasonal photometric variability of Titan, 1972–
411 2006. *Icarus* 200, 616-626.
412

413 Lora, J. M., Lunine, J. I., Russell, J. L. (2015). GCM simulations of Titan's middle and lower
414 atmosphere and comparison to observations. *Icarus* 250, 516–528.
415

416 Lorenz, E. N. (1955). Available potential energy and the maintenance of the general circulation.
417 *Tellus* 7, 157-167.
418

419 Lorenz, R. D., McKay, C. P. and Lunine, J. I. (1997). Photochemically driven collapse of Titan's
420 atmosphere. *Science* 275, 642-644.
421

422 Maltagliati, L. et al. (2015). Titan's atmosphere as observed by Cassini/VIMS solar occultations:
423 CH₄, CO and evidence for C₂H₆ absorption. *Icarus* 248, 1-24.
424

425 McCleese, D. J., Schofield, J. T., Taylor, F. W., Calcutt, S. B., Foote, M. C., Kass, D. M., Leovy,
426 C. B., Paige, D. A., Read, P. L. & Zurek, R. W. (2007). Mars Climate Sounder: An investigation
427 of thermal and water vapor structure, dust and condensate distributions in the atmosphere, and
428 energy balance of the polar regions. *Journal of Geophysical Research* 112, E05S06.
429

430 McCord, T. B. et al. (2004). Cassini VIMS observations of the Galilean satellites including the
431 VIMS calibration procedure. *Icarus* 172, 104-126.
432

433 McGrath M. A. et al. (1998). The ultraviolet albedo of Titan. *Icarus* 131, 382-392.
434

435 McKay, C. P., Pollack, J. B., Courtin, R. (1989). The thermal structure of Titan's atmosphere.
436 *Icarus* 80, 23–53.
437

438 McKay, C. P., Pollack, J. B. & Courtin, R. (1991). The greenhouse and antigreenhouse effects on
439 Titan. *Science* 53, 1118–1121.
440

441 Neff, J. S., Ellis, T. A., Apt, J. & Bergstralh, J. T. (1985). Bolometric albedos of Titan, Uranus,
442 and Neptune. *Icarus* 62, 425–432.
443

444 Newman, C. E., Lee, C., Lian Y., Richardson, M. I., Toigo, A. D. (2011). Stratospheric
445 superrotation in the TitanWRF model. *Icarus* 213, 636–654.
446

447 Pitman, K. M., Buratti, B. J., Mosher, J. A. (2010). Disk-integrated bolometric Bond albedos and
448 rotational light curves^[1] of saturnian satellites from Cassini Visual and Infrared Mapping
449 Spectrometer. *Icarus* 206, 537-560.
450

451 Porco, C. C. et al. (2004). Cassini Imaging Science: Instrument characteristics and anticipated
452 scientific investigations at Saturn, *Space Sci. Rev.* 115, 363-497.
453

454 Peixoto, J. P. & Oort, A. H. (1992). *Physics of Climate* (American Institute of Physics).
455

456 Read, P. L., Barstow, J., Charnay, B., Chelvaniththilan, S., Irwin, P. G. J., Knight, S., Lebonnois,
457 S., Lewis, S. R., Mendonça, J. & Montabone, L. (2016). Global energy budgets and ‘Trenberth

458 diagrams' for the climates of terrestrial and gas giant planets. *Quarterly Journal of the Royal*
459 *Meteorological Society* 142, 703-720.

460

461 Schubert, G. & Mitchell, J. L. (2013). Planetary atmospheres as heat engines. In *Comparative*
462 *Climatology of Terrestrial Planets* (Eds. Mackwell, S. J. et al.) (The University of Arizona Press).

463 Seignovert, B., Rannou, P., West, R. A., Vinatier, S. (2021). Haze seasonal variations of Titan's
464 upper atmosphere during the Cassini Mission. *The Astrophysical Journal* 907, 36.

465

466 Smith, P. H. (1980). The radius of Titan from Pioneer Saturn data, *J. Geophys. Res.* 85, 5943–
467 5947.

468

469 Smoluchowski, R. (1967). Internal structure and energy emission of Jupiter. *Nature* 215, 691-695.

470

471 Sohl, F., Sears, W. D., Lorenz, R. D. (1995). Tidal dissipation on Titan. *Icarus* 115, 278-294.

472

473 Spencer, J. R. & Nimmo, F. (2013). Enceladus: An active ice world in the Saturn system. *Annual*
474 *Review of Earth and Planetary Sciences* 41, 693-717.

475

476 Sromovsky, L. A. et al. (1981). Implications of Titan's north-south brightness asymmetry. *Nature*
477 292, 698-702.

478 Thomas, P. C. (2010). Sizes, shapes, and derived properties of the saturnian moons after the
479 Cassini nominal mission. *Icarus* 208, 395-401.

480

481 Tobie, G., Lunine, J. I., Sotin, C. (2006). Episodic outgassing as the origin of atmospheric methane
482 on Titan. *Nature* 440, 61-64.

483

484 Tomasko, M. G., Smith, P. H. (1982). Photometry and polarimetry of Titan: Pioneer 11
485 observations and their implications for aerosol proper- ties. *Icarus* 51, 65–95.

486

487 Tomasko, M. G., Bezdard, B., Doose, L., Engel, S., Karkoschka, E., Vinatier, S. (2008). Heat
488 balance in Titan’s atmosphere, *Planet. Space Sci.* 56, 648–659.

489

490 Toon, O. B., McKay, C. P., Griffith, C. A., Turco, R. P. (1992). A physical model of Titan’s
491 aerosols. *Icarus* 95, 24-53.

492

493 Trenberth, K. E., Fasullo, J. T., Von Schuckmann, K. & Cheng, L. (2016). Insights into Earth’s
494 energy imbalance from multiple sources. *Journal of Climate* 29, 7495-7505.

495

496 West, R. et al. (2010). In-flight calibration of the Cassini imaging science sub-system cameras.
497 *Planetary and Space Science* 58, 1475-1488.

498

499 West, R.A., Seignovert, B., Rannou, P., Dumont, P., Turtle, E. P., Perry, J., Roy, M. and
500 Ovanessian, A. (2018). The seasonal cycle of Titan's detached haze. *Nature Astronomy* 2, 495-
501 500.

502

503 Willson, R. C., Mordvinov, A. V. (2003). Secular total solar irradiance trend during solar cycles

504 21–23. *Geophysical Research Letters* 30.

505

506 Yang, S. K., Hou, Y. T., Miller, A. J., Campana, K. A. (1999). Evaluation of the earth radiation
507 budget in NCEP–NCAR reanalysis with ERBE. *Journal of climate* 12, 477-493.

508

509 Younkin, R. L. (1974). The albedo of Titan. *Icarus* 21, 219–229.

510

511 Zebker, H. A., Stiles, B., Hansley, S., Lorenz, R., Kirk, R. L. & Lunine, J. (2009). Size and shape
512 of Saturn’s moon Titan. *Science* 324, 921–923.

513

514

515 **Figure Captions**

516

517

518 **Figure 1.** Titan’s Bond albedo from 2004-05 to 2017. Vertical lines represent measurement
519 uncertainties. There are only three months (October-December) of high-quality observations in
520 2004, so the 2004 observations are combined with the 2005 observations.

521

522

523 **Figure 2.** Titan’s total solar power, reflected power, and absorbed solar power from 2004-05 to
524 2017. (A) Total solar power over Titan. (B) Total solar power reflected by Titan. (C) Total
525 absorbed power absorbed by Titan. Vertical lines in the three panels represent measurement
526 uncertainties.

527

528

529 **Figure 3.** Comparison between Titan’s absorbed solar power and emitted thermal power during
530 the Cassini epoch. (A) Comparison between the absorbed solar power (red line) and the emitted
531 thermal power (blue line). The measurements of Titan’s emitted power are from our previous study
532 (20). (B) The ratio between the net radiant energy (i.e., absorbed power – emitted power) and the
533 emitted power. The horizontal dashed line is the reference line with the ratios equating zero. The
534 vertical lines in the two panels represent measurement uncertainties.

535

536

537

538

539

540

541

542

543

544

545

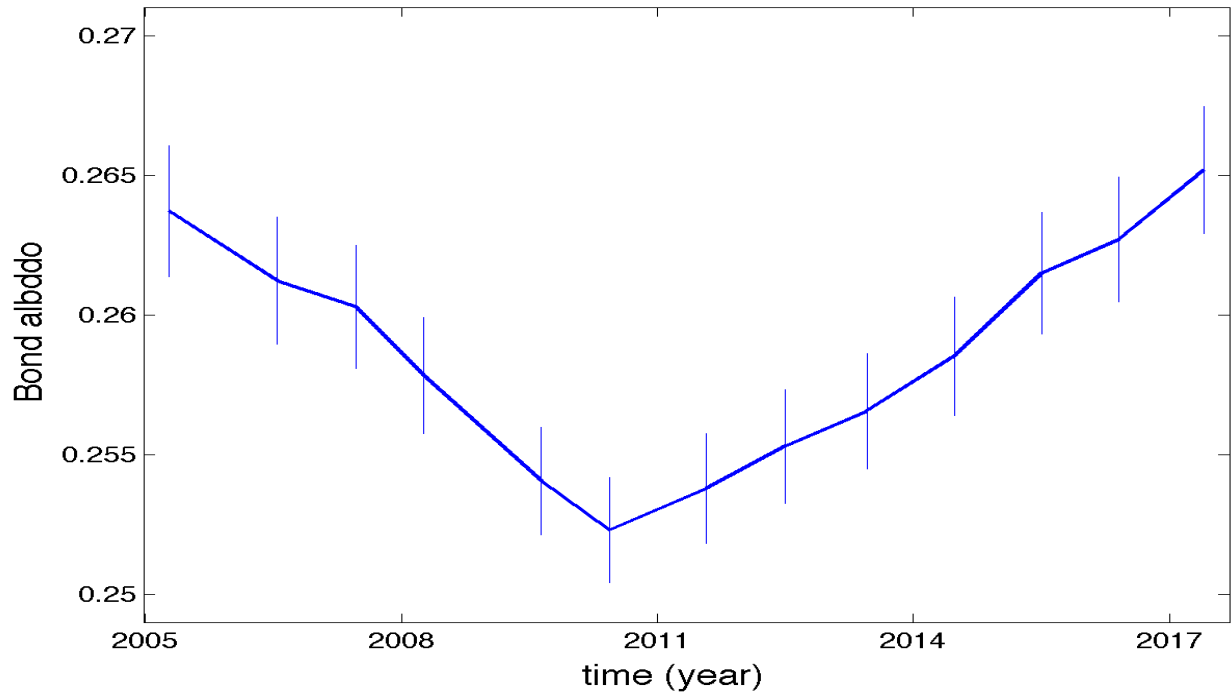
546

547 Figure 1

548

549

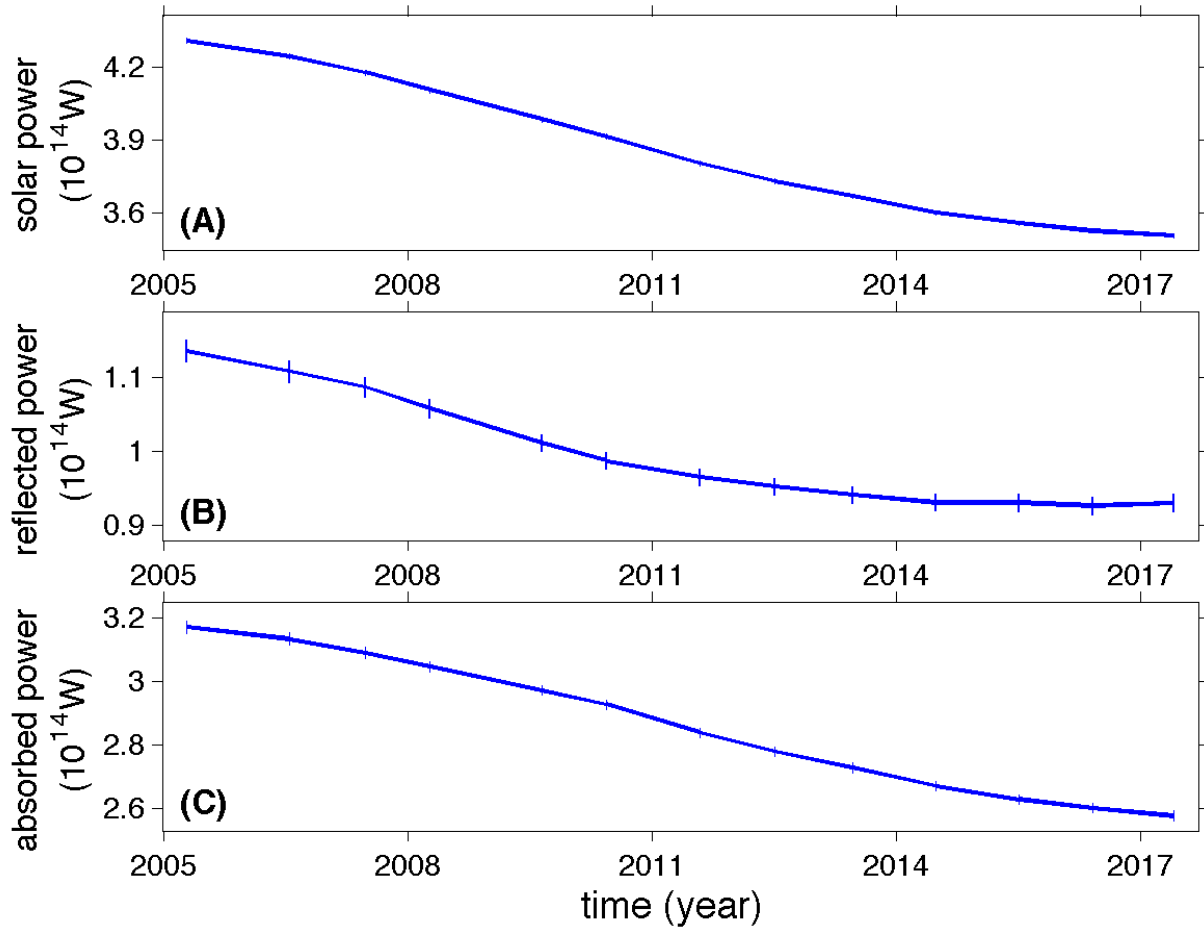
550



551
552
553
554
555
556
557
558
559
560
561
562
563
564
565
566
567
568
569
570
571
572
573

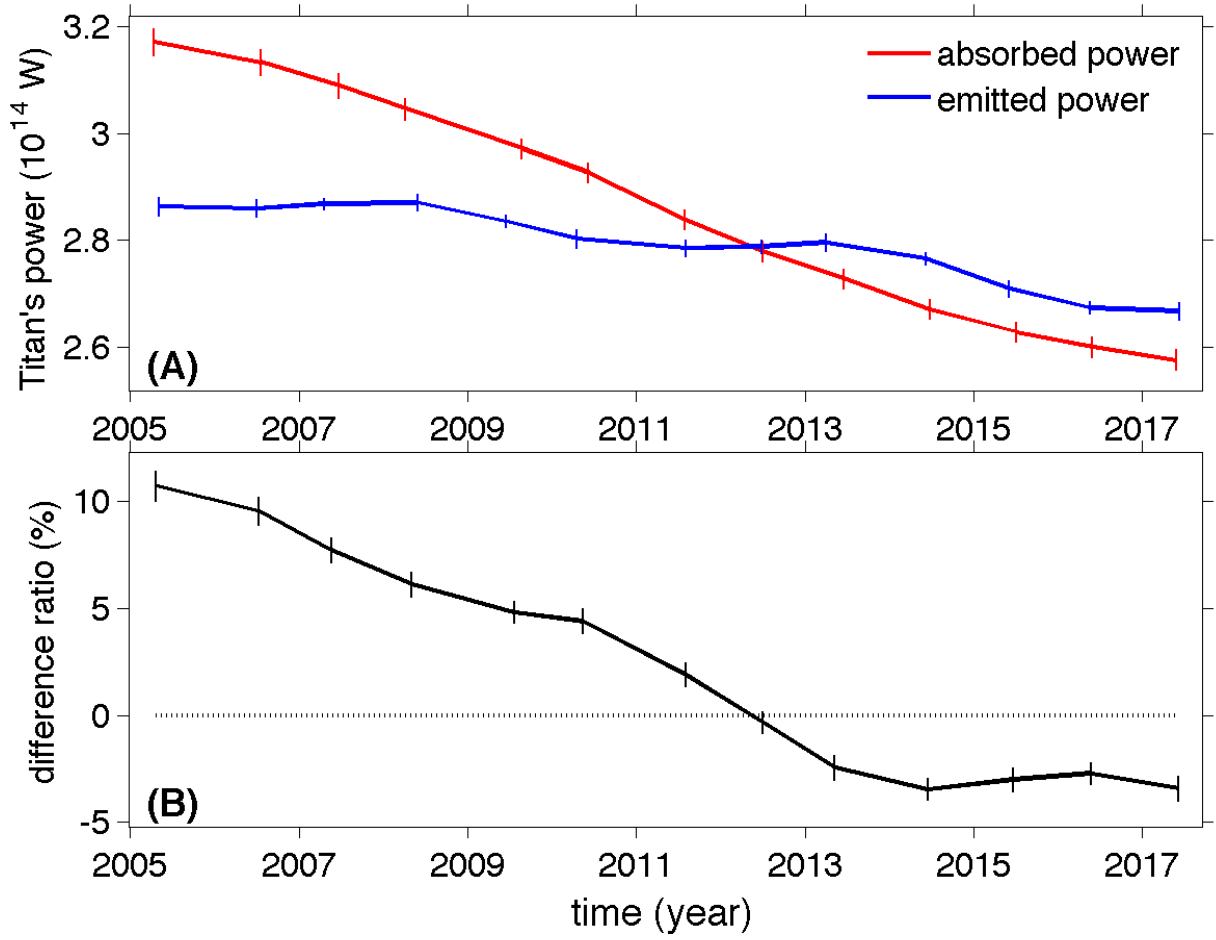
Figure 2

574
575
576
577
578



579
 580
 581
 582
 583
 584
 585
 586
 587
 588
 589
 590
 591
 592
 593
 594
 595
 596
 597
 598
 599
 600

Figure 3



601
602